

Electron beam pointing instability in a self-injected laser wakefield accelerator

S P D Mangles, M C Kaluza, A G R Thomas, C D Murphy*, Z Najmudin, A E Dangor, K Krushelnick

The Blackett Laboratory, Imperial College London, Prince Consort Road, London, SW7 2BW, UK

* also at Central Laser Facility, CCLRC Rutherford Appleton Laboratory, Chilton, Didcot, Oxon., OX 11 0QX, UK

P S Foster, C J Hooker, A J Langley, E J Divall, K G Ertel, J M Smith

Central Laser Facility, CCLRC Rutherford Appleton Laboratory, Chilton, Didcot, Oxon., OX 11 0QX, UK

Main contact email address: stuart.mangles@imperial.ac.uk

Introduction

Laser driven accelerators using plasma waves as the accelerating medium offer the possibility of compact sources of electrons, x-rays and THz radiation¹⁻³). Recent progress in this field has generated significant interest due to the observation of quasi monoenergetic features in the electron energy spectrum produced due to wavebreaking in a laser-wakefield accelerator⁴⁻⁶).

However the control and stability of these electron beams remains a serious concern. All groups report a degree of shot-to-shot variation in the measured electron beam parameters including beam charge, beam energy and beam energy spread, that is unacceptable for use in most applications. Most of the fluctuation can be attributed to variations in the laser parameters, including focal spot intensity distribution, pointing, pulse energy and pulse duration.

In this article we report the observation of an electron beam pointing instability in a laser wakefield accelerator may be important for the future application of such beams.

During the same experiment it was also found that the laser beam was undergoing a long wavelength hosing instability. This was observed in the image of self-scattered laser light from the plasma. Although the occurrence of hosing has previously been inferred from the effect on plasma channels left behind a long (~ 1 ps) pulse⁷), this measurement represents the first direct observation of long wavelength hosing of a short ($c\tau \sim 2\pi/\omega_p$) pulse in a plasma.

Experimental Set-up

The experiment was performed with the 10 TW Astra laser. During this experiment the laser pulse energy was approximately 300 mJ on target with FWHM duration of 40 fs. The laser beam was focused onto the edge of a 2 mm supersonic helium gas jet with a 1 m focal length, $f/16$ off axis parabolic mirror.

The electron beam produced in the experiment was measured using an on-axis magnetic electron spectrometer. Electrons are deflected away from the laser axis by the electromagnet onto an image plate detector⁸) which provides a high-resolution, single-shot electron spectrum measurement over a reasonable range of energies (approximately 10 – 150 MeV).

The interaction was also imaged from the side by a high-resolution $f/2$ achromatic lens onto a 12 bit CCD camera. An 800 ± 10 nm interference filter ensured that the image was dominated by scattering of the laser beam by the plasma.

The electron beam profile was also measured (although not simultaneously with the electron spectrum) by placing a scintillating LANE screen on the laser axis. The light emitted from the screen was imaged onto a 10-bit CCD camera. To allow the beam profile of the high-energy electrons to be measured the screen was placed behind a 15 mm aluminium sheet, with a further 2 mm of lead shielding to limit the electron energies incident on the screen to $E > 11$ MeV. The scattering induced by this shielding was estimated using the theory of Molière⁹) and was found to increase the apparent beam size on

the screen by less than 1 mm for 100 MeV electrons and as much as 8 mm for 11 MeV electrons.

A far-field monitor was set up to measure the laser beam stability during the experiment. The small amount of light which leaked through the back of one of the dielectric mirrors in the interaction chamber was transported out of the chamber through a window and focused. An 8-bit CCD camera with a microscope objective was used to image this focal spot. Although this focal spot is not a replica of the actual focal spot in the interaction chamber, variations in the recorded image from shot-to-shot will be representative of the transverse variations of the actual focal spot.

Experimental Results

Figure 1 shows a number of measured electron spectra measured at various plasma densities. The horizontal axis represents the electron energy and the vertical axis represents the transverse dimension of the electron beam inside the spectrometer.

During this experiment narrow energy spread features were observed in the spectrum of the electron beam, although the electron energy was lower than in previous Astra experiments⁴). This is most likely due to the fact that the laser energy was lower during this experiment.

At a density of $n_e = 1 \times 10^{19} \text{ cm}^{-3}$ narrow energy spread features were consistently observed. Figures 1 and 2 show four spectra indicating the degree of shot-to-shot variation. There were also shots (approximately 1 in 5) where no measurable electron signal was produced in the electron spectrometer.

At $n_e = 1 \times 10^{19} \text{ cm}^{-3}$ the highest energy narrow energy spread features appeared near 20 - 30 MeV reasonably consistently. The transverse profile of the spectrum (Figure 1) shows that the 30 MeV beam was either narrower than the spectrometer slit (Figure 1a) or that the beam was moving laterally between shots.

Figure 3 shows nine typical measurements of the electron beam profile above 11 MeV. During this experiment the pointing of electron beam was clearly unstable. The electron beam profile also exhibits multiple beamlets on a significant number of shots.

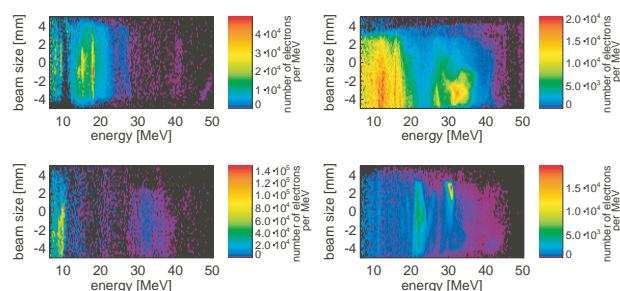


Figure 1. Measured electron spectrum at $n = 1 \times 10^{19} \text{ cm}^{-3}$ showing shot-to-shot variation. The x-axis is the electron energy and the y-axis is the beam size inside the spectrometer. The projection of the collimator onto the detector is approximately 8 mm.

Figure 4 shows the position of the electron beam of a number of shots. The data presented includes only shots where a single, well-defined beam was observed. Out of a run of 56 shots only 12 fulfilled this criteria with 10 shots showing no measurable electron signal, consistent with the results from the electron spectrometer measurement.

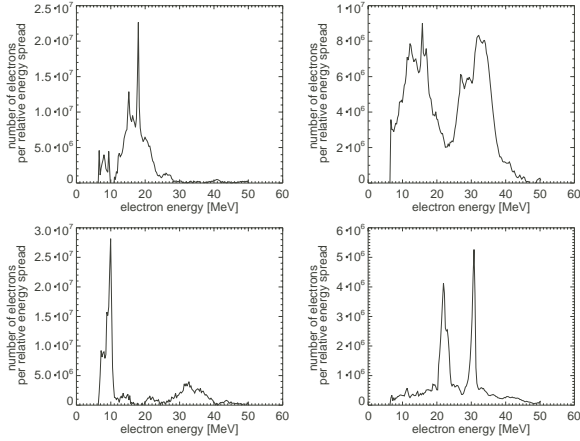


Figure 2. Electron Spectra integrated across the image plate for the data presented in Figure 1.

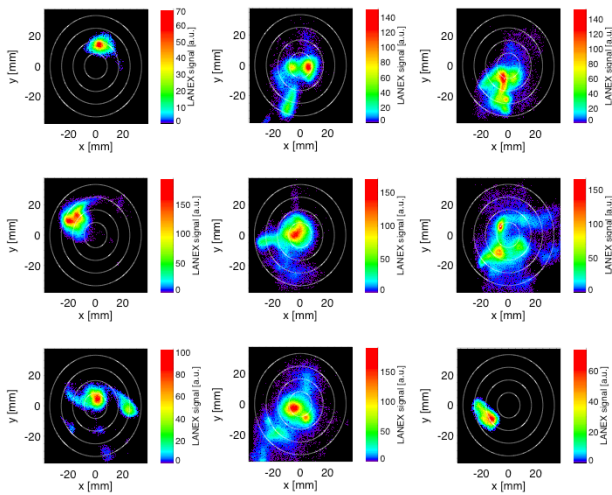


Figure 3. Electron beam profile ($E > 11$ MeV) measured on the LANEX screen at a plasma density of $n_e = 1 \times 10^{19} \text{ cm}^{-3}$ for 9 shots under the same conditions. The screen was 48 cm from the interaction. Contours at 1° , 2° , 3° and 4° are indicated.

The most obvious potential cause for the electron beam pointing instability would be the pointing stability of the laser itself. Figure 5 shows the laser focal spot stability measured in the target close to the interaction recorded during a run of 31 shots. Figure 5a) shows the laser pointing during these shots, normalized to the average spot size w_0 . The RMS deviation of the laser pointing is less than $0.2 w_0$, this pointing deviation corresponds to less than 0.02° (0.3 mrad).

As well as the laser pointing the far-field monitor allows changes in the focal spot size and asymmetry to be monitored. We measure the spot width by integrating the focal spot image in either the x or y direction and fitting a gaussian function to the resulting profile. The spot asymmetry is then defined as the ratio of the spot waist in x and y , i.e. w_x/w_y .

Since the far-field monitor is not an exact replica of the actual focal spot it is only changes in the spot size and asymmetry that are of interest. The RMS deviation of the spot asymmetry was

measured to be approximately 40% which may be significant in terms of the seeding of instabilities in the plasma.

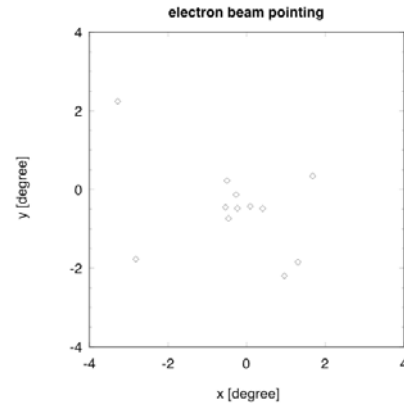


Figure 4. Electron beam pointing stability.

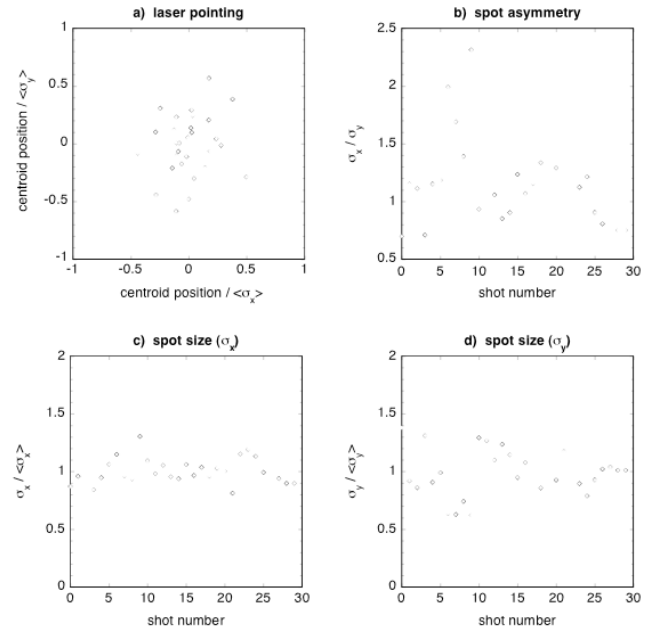


Figure 5. Shot-to-shot variations in the laser far-field.

One such instability that could be seeded by focal spot asymmetry is laser hosing. This was observed using the side imaging system which observed the self-emission (at 800 nm). The amount of side emission decreased below the detection threshold for the plasma densities where the electron beam profile measurements were made, however side images were obtainable at higher densities. These images show direct evidence of a long wavelength hosing instability.

Figure 6 show two separate observations of this long wavelength hosing. Figure 6 a) shows the self-emission from the channel at a density of $n_e = 2.8 \times 10^{19} \text{ cm}^{-3}$. The wavelength of this hosing is approximately $65 \mu\text{m}$, which corresponds to approximately ten relativistic plasma wavelengths ($\lambda_p = 2\pi c/\omega_p$). Figure 6 b) shows the same image with the channel centroid clearly marked with a white line. Figure 6 c) and 6 d) show another channel at lower density of $n_e = 1.6 \times 10^{19} \text{ cm}^{-3}$. Once again there is clear evidence of the laser hosing as it travels through the plasma. The wavelength of

this hosing motion at this lower density is longer, being approximately $125 \mu\text{m}$, corresponding to approximately $10 \lambda_p$.

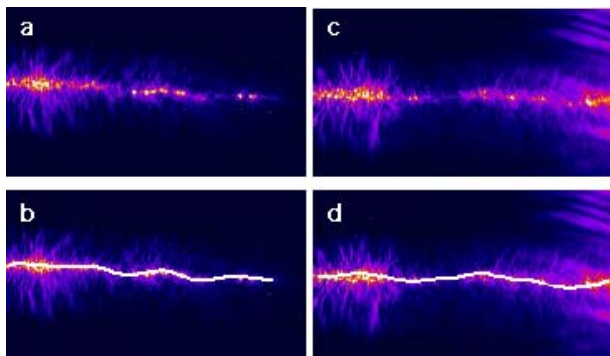


Figure 6. Images of the self-emission from the plasma channel at 800 nm at **a)** and **b)** $n_e = 2.8 \times 10^{19} \text{ cm}^{-3}$. **c)** and **d)** $n_e = 1.6 \times 10^{19} \text{ cm}^{-3}$.

The intensity of the self-emission from plasma densities near $n_e = 1 \times 10^{19} \text{ cm}^{-3}$ was insufficient to produce a good quality image using the image system employed, so that it is not possible to state unequivocally that this hosing was also occurring at the plasma density at which the electron beam pointing instability was observed. However it is highly likely that this hosing did occur at lower densities and that this had an effect on the observed electron beam pointing.

To our knowledge the observed hosing is markedly different from any reported observations of hosing in either experiment⁷⁾ or simulations e.g. reference¹⁰⁾. This is due to the fact that the wavelength is much longer than the pulse length, $c\tau \approx 12 \mu\text{m}$. With long pulses the hosing occurs within the pulse, i.e. along the pulse there are deviations of the pulse centroid. In this short pulse regime the centroid of the entire pulse must be deviated by the same amount at each point in time.

Although the laser hosing is a potential cause for the observed electron beam pointing instability observed there is an alternative explanation. It is known that after the electron bunch has been injected into the accelerating plasma wave the transverse (focusing) forces associated with the plasma wave can lead to so-called betatron oscillations, the x-ray emission from this motion has been observed previously¹¹⁾. If the electron bunch is indeed performing betatron oscillations in the plasma wave then the phase of the bunch in this oscillation at the point when it leaves the plasma will determine the angle at which the electron beam travels.

No evidence for betatron motion was observed during the experiment. If such motion was occurring then we might expect to observe an x-ray signal on the axis of the spectrometer. The image plate detectors used measured no such signal during this experiment, although this may simply be due to the relatively small charge in the electron beam during this experiment ($\sim 1 \text{ pC}$).

The electron beam pointing instability and the laser hosing are clearly potentially serious issues for the stability of laser-plasma based accelerators. If both are indeed seeded by the focal quality of the laser beam then this may be controllable through the use of, for example, adaptive optics. Recent simulations¹²⁾ have suggested that in the ‘‘bubble regime’’ of electron acceleration¹³⁾ long interaction lengths can be achieved without the need for external guiding mechanisms, however it may be the case that external guiding helps to stabilise laser-produced electron beams.

References

1. T Tajima and J M Dawson, Phys. Rev. Lett. **43**, 267-270, (1979)
2. E Esarey *et al.*, Nucl. Instrum. Methods A, **331**, 545-549 (1993)
3. W P Leemans *et al.*, Phys. Rev. Lett. **91** 074802 (2003)
4. S P D Mangles *et al.*, Nature **431**, 535-538 (2004)
5. C G R Geddes *et al.*, Nature **431**, 538-541 (2004)
6. J Faure *et al.*, Nature **431**, 541-544 (2004)
7. Z Najmudin *et al.*, Phys. Plasmas **10**, 438-442, (2003)
8. K A Tanaka *et al.*, Rev. Sci Instrum **76**, 013507 (2005)
9. S Eidelman *et al.*, Phys. Lett. B. **592**, 1-1109 (2004)
10. B J Duda *et al.*, Phys. Rev. Lett. **83**, 1978-1981 (1999)
11. K T Phuoc *et al.*, Phys. Plasmas **12**, 023101 (2005)
12. W B Mori, Private communication (2005)
13. A Pukhov and J Meyer-ter-Vehn Appl. Phys. B **74**, 355 (2002)